Fabrication of Gold Nanoparticles using Andrographis Paniculata Leaf Extract and its Potentiality against Plant Pathogens

P. Viji and P. Prema

Research Journal of Agricultural Sciences
An International Journal

P- ISSN: 0976-1675
E- ISSN: 2249-4538

Volume: 13
Issue: 03

Res. Jr. of Agril. Sci. (2022) 13: 843–848

CARAS

Res. Jr. of Agril. Sci. (May-Jun 2022)
13(3): 843–848

ISSN: 0976-1675 (P)
ISSN: 2249-4538 (E)

www.rjas.org

Full Length Research Article

Fabrication of Gold Nanoparticles using *Andrographis* Paniculata Leaf Extract and its Potentiality against Plant Pathogens

P. Viji[1] and P. Prema*[2]

Received: 03 Apr 2022 | Revised accepted: 12 Jun 2022 | Published online: 17 June 2022

A B S T R A C T

The significance of gold nanoparticles (AuNPs) against diverse plant pathogens is nowadays perfectly established in the field of agriculture. The present study focused to examine the antimicrobial efficiency of green synthesized gold nanoparticles against selected plant pathogens like *Aspergillus flavus*, *Aspergillus niger* and *Pseudomonas syringae.* The synthesized AuNPs were characterized by UV-visible, FTIR, XRD spectroscopy, SEM, EDX, DLS and zeta potential studies. The AuNPs exhibited a surface Plasmon resonance (SPR) peak at 528 nm. The FTIR spectrum revealed the contribution of bioactive compounds in the leaf extract for the reduction process as well as stabilization of AuNPs. The XRD spectrum of AuNPs explains the crystalline nature of the synthesized gold nanoparticles. The SEM image showed the morphology and shape of the nanoparticles. The elemental analysis of the synthesized AuNPs was found using energy dispersive spectrum. The size of the AuNPs was measured in DLS and it was 55.6 ± 19.4 nm with a polydispersity index of 0.212. The zeta potential value observed for gold nanoparticle was -42 mV which indicates the stability of the nanoparticle. The obtained inhibitory zone observed in the present study for selected plant pathogens revealed the resultant gold nanoparticles have good potentiality against infectious diseases in plants. The MIC was found to be significant with IC50 values of 14.19, 14.08 and 18.07 µg/ml respectively.

***Key words*:** AuNPs, Plant pathogen, *A. flavus, A. niger, P. syringae,* Antimicrobial, MIC

Nanoscience is a new field of scientific inquiry that has gained a lot of attention in recent decades [1]. Nanotechnology can create new design and manipulation of nanostructures with extremely small dimensions and high surface area to volume ratios which play a crucial role in microbiology and biotechnology. Nanoparticles have caught the great attention of researchers from a wide range of fields due to their unique features. Nanoparticles are classed on the basis of their morphology, size, and chemical properties, and so they are classified according to their physical and chemical qualities; there are various well-known kinds of nanoparticles such as organic, inorganic, and carbon-based [2].

Agricultural damage is due to phytopathogens which contribute for around 6% of crop yield production around the world [3]. The losses incurred by these infections are undeniable, and they can be exacerbated even more dependent on predisposing factors, pathogen virulence, and the surroundings. Regardless of the fact that weeds are the largest source of yield losses on a worldwide scale, agricultural crops suffer significant losses due to insect infestations and plants infections by bacteria and fungi. In the twenty-first century, the global annual production tonnage percentage lost due to diversified pests was approximated as follows in rounded (approximate) figures: Animal pests were responsible for 18% of crop production tonnage losses; illnesses caused by microbes which accounted about 16% and 70-80% crop losses are owing to fungal pathogens; 34% loss for a total of 68% annual crop production due to the presence of weeds in the surrounding environment [4].

Aspergillus flavus is a soil fungus which mainly infect plants, animals and insects. It grounds storage rots disease in numerous crops such as corn, peanuts and cotton. It also causes an ear rot disease in corn [5] yellow mould in peanut seedlings [6] and yellow spot disease that affects the quality of cotton fibre [7]. *Aspergillus niger* is also a causative agent for many rot diseases in plants. It causes substantial economic losses in food products due to spoilage. It produces crown rot disease in peanuts [8], spoilage in grapes [9] and tomatoes [10] during storage. *Pseudomonas syringae* is a phytopathogen which causes diseases of monocots, woody dicots and herbaceous plants throughout the world. Recently nanoparticles can safeguard the plants by implementing dual protocols such as nanoparticles itself fostering the protective effect on agricultural crops and nanoparticles acts as carriers for active compounds as well as in combination with pesticides [11]. Hence, the present research aims to find the whole aspects about green synthesis of gold nanoparticles and its potential

* **P. Prema**
✉ prema@vhnsnc.edu.in

[1-2] Department of Zoology, V.H.N. Senthikumara Nadar College, Virudhunagar - 626 001, Tamil Nadu, India

antimicrobial efficacy against plant pathogens to develop new therapeutics for the protection of agricultural crops.

MATERIALS AND METHODS

Gold (III) chloride trihydrate ($HAuCl_4$. $3H_2O$) was purchased from HiMedia, Chennai. The gold chloride stock solution (1mM; w/v) was prepared by dissolving 39.383mg of gold (III) chloride trihydrate in 100ml Type I water (Water Purification System Model Direct-Q3, Bangalore, India). All glasswares used in the present work was thoroughly rinsed with deionized water.

Andrographis paniculata leaf extract preparation

The young and fresh *Andrographis paniculata* leaves were collected in the district of Tirunelveli, Tamil Nadu, India. The collected leaves were washed thrice in de-ionized water, and then shade-dried for one week. The dried leaves were crushed using mixer grinder and sieved and kept in air tight container for further analysis. 10g of dried fine powdered leaves in suspended in 100 ml of Milli-Q water and boiled at 100°C for 10 minutes. Using Whatman No. 1 filter paper, the slurry was filtered and kept in refrigerator at 4°C for subsequent research work.

Fabrication of AuNPs using AP leaf extract

For the fabrication of AuNPs, 1mM gold chloride solution (w/v) was prepared from commercially procured tetrachloroauric acid salt. 100ml gold chloride solution was taken in a 250 ml Erlenmeyer flask and heated to 80°C for 10 minutes. The solution was then agitated for 15 minutes at 80°C for 400 rpm. Then, 10ml of 10% (w/v) *Andrographis paniculata* leaf extract was added in a dropwise manner. The colour change from pale yellow to ruby red in the reaction mixture which indicates the formation of gold nanoparticle. After the fabricated AuNPs was centrifugated at 8000 rpm for 20 minute and the top most fluid was drained off. The obtained precipitate was washed multiple times with type I water and dried at 50°C in hot air oven.

Characterization of gold nanoparticles

The fabricated gold nanoparticle was measured using UV-vis spectrum at 1nm resolution and type I water as reference using a Shimadzu dual beam spectrophotometer (model UV – 1800 PC) with a wavelength from 200 nm to 800 nm [12]. The synthesized AuNPs was performed using Fourier transform infra-red spectroscopy with a range of 4000–400 cm^{-1} in Nicolet Impact 400 FT-IR spectrophotometer [13]. The X-ray diffraction analysis for the crystalline nature of AuNPs was determined using an X'pert PROPAN analytical instrument. The obtained diffraction intensity peaks were compared with the standard Joint Committee for Powder Diffraction Standard (JCPDS) files [14]. The size and morphology of synthesized AuNPs was determined using scanning electron microscope (SEM). DLS (Dynamic light scattering) and zeta potential of the AP-AuNPs was determined using Zeta sizer-SZ100 (Horiba, Japan) to measure the average size, zeta potential and polydispersity index of green synthesized AuNPs.

Antimicrobial activity

The antimicrobial activity of green synthesized AuNPs was evaluated using the selected plant pathogens, including two fungus strains such as *Aspergillus flavus* (MTCC 277), *Aspergillus niger* (MTCC 404) and bacterial strain *Pseudomonas syringae* (MTCC 7620). The overnight grown pathogens were swabbed on Mueller Hinton Agar (MHA) plates. The AP-AuNPs with four different concentrations (50, 100, 150 and 200 µg/ml) were dispensed into the agar wells in the petri plates made using cork borer. Then the petri plates were kept overnight at 37°C. The inhibitory zone was assessed and this study was done in five individual replicates. The minimum inhibitory concentration of AP-AuNPs were determined by broth dilution method using 96 well plate. The two-fold dilutions were made for each sample at various concentrations and maintained overnight at room temperature. A control was also maintained for each experiment. The optical density of bacterial growth (OD) values at 630 nm using ELISA plate reader (ERBA, LisaScan) growth. The inhibition of growth in the sample loaded wells for each dilution was calculated using the following formula:

$$\text{Inhibition (\%)} = \frac{OD\ of\ control - OD\ of\ test\ sample}{OD\ of\ control} \times 100$$

Statistical analysis

The observed data are expressed in Mean ± SD. The one-way ANOVA and post hoc analysis were carried out using Minitab software version 17. The statistically significant inferences are expressed in $p<0.05$ and $p<0.001$.

RESULTS AND DISCUSSION

Characterization of AuNPs

(Fig 1) shows the transformation of colour of the green synthesized gold nanoparticle from golden yellow to wine red colour. Correspondingly, the colloidal AuNPs synthesized by *Mentha longifolia* leaf extract was also wine red colour [15]. In contrast, the gold nanoparticle synthesized by chemical method using tri sodium citrate as reducing agent showed reddish purple colour [16]. The ultra violet -visible spectrum of AP-AuNPs and its intense absorption peak was recorded at 528 nm is illustrated in (Fig 2). Saqr *et al.* [17] reported that the absorption peak was around 525-555 nm. Analogously, Balasubramanian *et al*. [18] stated that the intensity peak value at 547 nm for gold nanoparticles fabricated using *Jasminum auriculatum* plant leaf extract.

Fig 1 Visible colour change in the reaction mixture of AuNPs

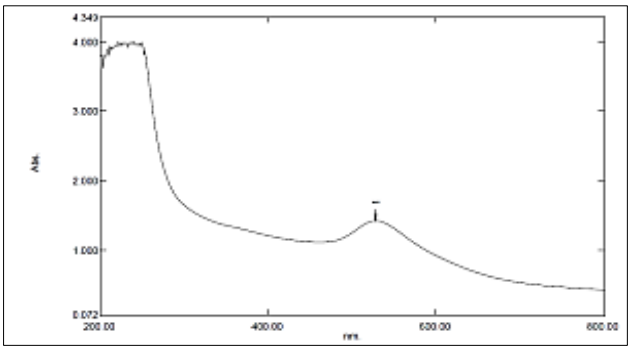

Fig 2 UV-visible spectrum of synthesized AuNPs

The FTIR spectrum obtained from AP-AuNPs in (Fig 3) depicts that the stretching bands ranged from 1000 to 3800 cm^{-1} which implies the occurrence of O-H vibration and the existence of functional groups such as free hydroxyl, N-H stretch denotes primary and secondary amines and amides, which resembles the earlier reports [19-20]. The stretching vibration at 2881.13 cm^{-1} indicates the presence of O-H stretch carboxylic groups and the region of 2634.29 cm^{-1} indicates the H-C=O; C-H stretch as aldehyde group. The C=C stretching alkene vibration band appeared at 1683.55 and 1292.07cm^{-1} showed C-H wagging in AP-AuNPs, which corroborates with a previous study [21]. The stretching occurs at, 1028.84 and 958.44cm^{-1} which indicates the C-N stretch of aliphatic amines groups and O-H stretch with carboxylic acids as functional group.

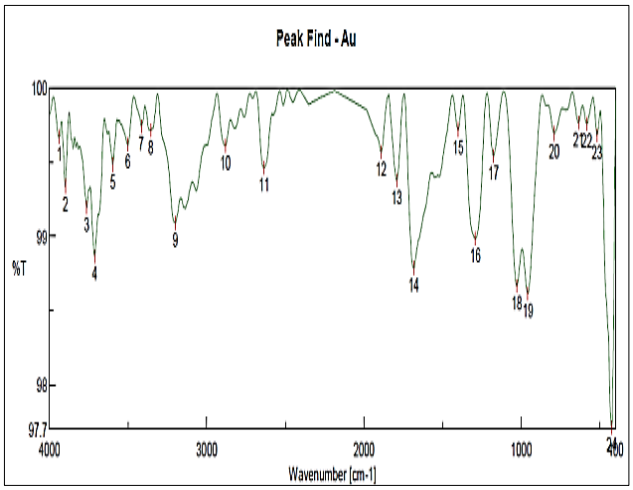

Fig 3 FTIR spectrum of synthesized AuNPs

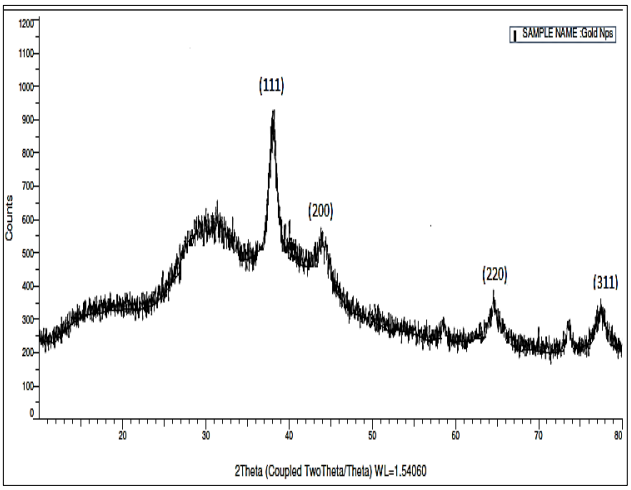

Fig 4 XRD pattern of synthesized AuNPs

XRD pattern of the *A. paniculata* mediated gold nanoparticles, which was crystalline in nature and an intense peak proved the structure of AP-AuNPs (Fig 4) to be face centered cubic (FCC) nature including 38.16°, 44.00°, 65.3°, and 73.53° (111, 200, 220 and 311 respectively) and the obtained data was compared with JCPDS file (No. 00-004-0784). The recorded XRD pattern of AuNPs is coherent with the existence of its metallic gold constituents as reported earlier [22-24].

The SEM image of AP-AuNPs synthesized is represented in (Fig 5). It revealed that the gold nanoparticles are completely dispersed and the leaf extract worked as the crowning agent to form discrete AuNPs from accumulation. The size of the AuNPs was between from 40 to 65 nm and most of them were spherical in shape. The present result relates the earlier report [25] and they explained the shape of the nanoparticles were roughly spherical in shape and in some areas stacked together. The EDX analysis confirmed the presence of metallic Au in the synthesized gold nanoparticles with a range between 2-2.5keVis illustrated in Fig.6. In accordance with earlier reports [26] suggested that the energy band for Au shows a strong signal in the range of 2 to 2.5keV.

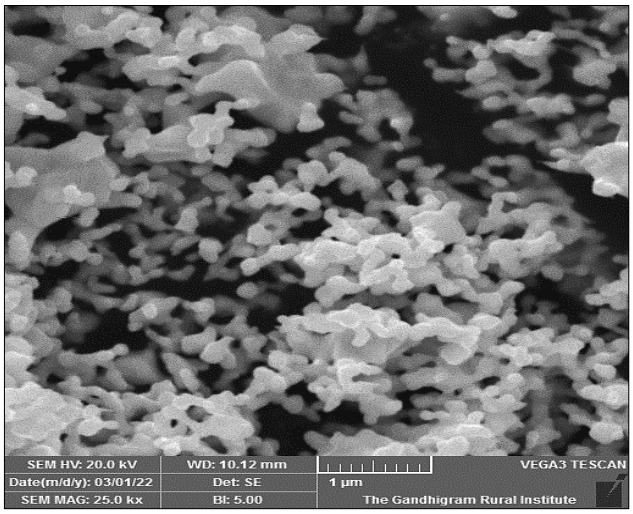

Fig 5 SEM image of AuNPs

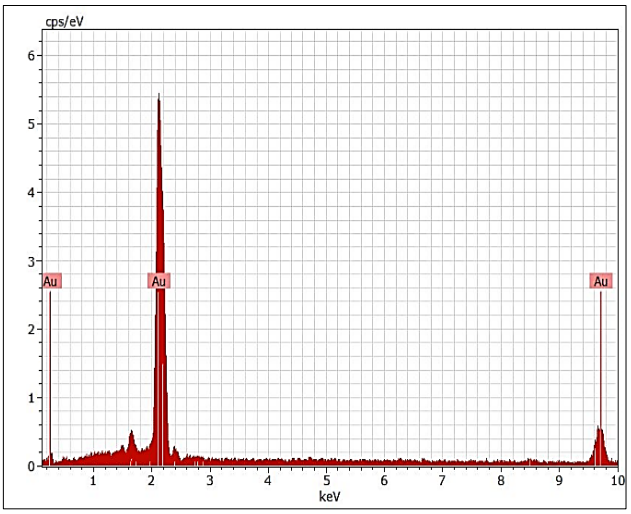

Fig 6 EDX spectrum of AuNPs

Dynamic light scattering detects the size of biosynthesized particle to be between 40 and 65 nm with a standard deviation of 19.4 nm (Fig 7). The z- average of AuNPs was 47.2 nm in the synthesis process with a poly dispersity index of 0.212. Keskin *et al*. [26] reported that the *Gundelia tournefortii* leaf extract mediated gold nanoparticle exhibited 146 nm in size. The zeta potential of the AP-AuNPs was found to be -42.0 mV (Fig 8) with a good stability index. The data obtained in the present study have a negative zeta potential as proved owing to the occurrence of negatively charged functional groups in the leaf extract which offers more stability of synthesized gold nanoparticles [27]. Adena *et al.* [28] reported that the surface charge of metallic Au nanoparticle have shown to be more stable if it is either more -30 or +30.

Antibacterial and antifungal activity

The antibacterial and antifungal efficacy of biosynthesized AP-AuNPs was analyzed with selected pathogenic microbial strains by agar well diffusion method. The bacterial strains selected in the study was *Pseudomonas syringae* and fungal strains such as *A. flavus* and *A. niger*. The zone of inhibition for the selected plant pathogens is given in (Fig 9-10). It shows that the higher concentration (200 µg/ml) gave better performance than the lower concentration (50 µg/ml). The standard antibiotic(30µg/ml) Clotrimazole exhibited better antifungal effect (24 and 19 mm) to *A. flavus* and *A. niger* respectively than the AP-AuNPs (22.66 ± 0.57 and 15.00 ± 0.81 mm) at 200 µg/ml as the standard antibiotic which possess the chemical compound exclusively to inhibit the growth. Likewise, for the bacterial strain, Azithromycin was used as standard which showed zone of inhibition (25mm) and AP-AuNPs with 22.66 ±0.47 mm at the highest concentration. The obtained result revealed that the increasing AuNPs concentration gives diminishing growth of microbial cells in a dose dependent manner.

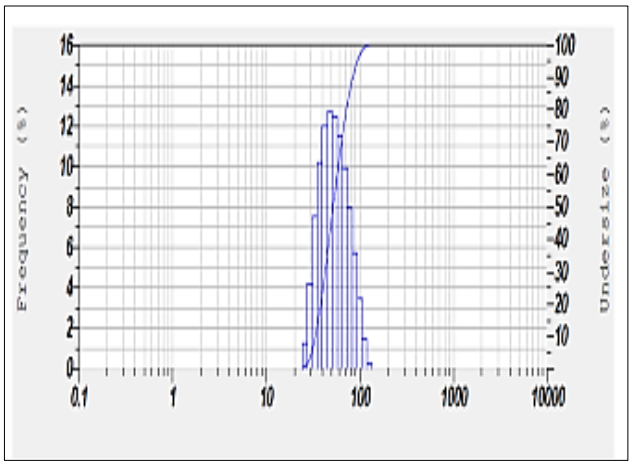

Fig 7 Particle size of synthesized AuNPs

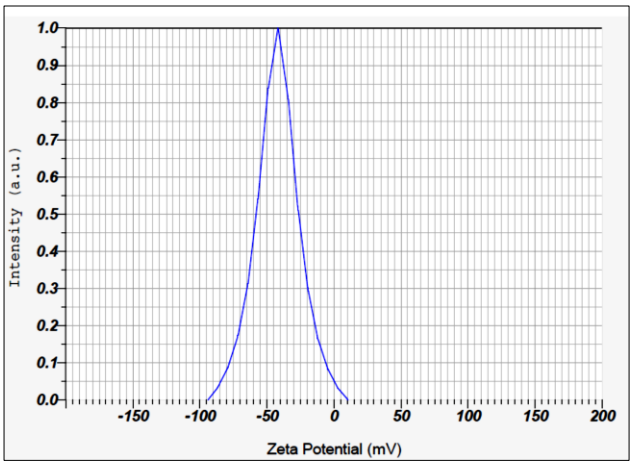

Fig 8 Zeta potential of synthesized AuNPs

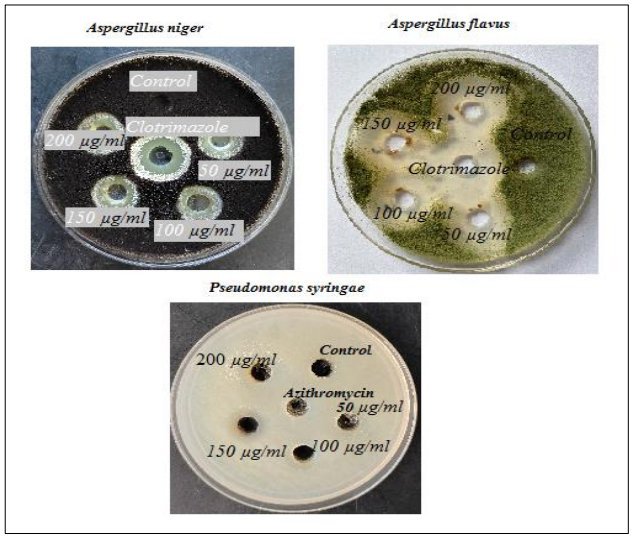

Fig 9 Photograph showing antimicrobial activity against plant pathogens

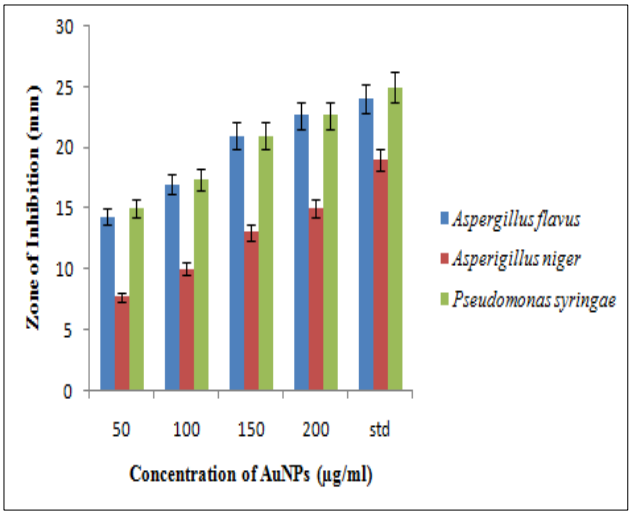

Fig 10 Zone of Inhibition (mm) of AuNPs

Table 1 Zone of inhibition in mm using AuNPs against plant pathogens. Each value is the mean±SD of three individual replicates. Different superscript alphabets are statistically significant from each other (Post hoc Tukey test; P<0.001)

Plant pathogen	Concentration (µg/ml)				
	50	100	150	200	Standard
A. flavus	14.33 ± 0.57^{d}	17.00 ± 1.00^{c}	21.00 ± 1.00^{b}	22.66 ± 0.57^{ab}	24^{a}
A. niger	07.66 ± 0.47^{d}	10.00 ± 0.81^{c}	13.00 ± 0.81^{b}	15.00 ± 0.81^{b}	19^{a}
P. syringae	15.00 ± 0.81^{d}	17.33 ± 0.47^{c}	21.00 ± 0.81^{b}	22.66 ± 0.47^{b}	25^{a}

The metallic gold nanoparticle was shown to be good antimicrobial efficiency against plant fungal pathogens such as *A. flavus* and *A. niger* as well as plant blight disease causing bacterial strain, *Pseudomonas syringae*. These findings support the previous studies [29-30] stated that the metal nanoparticles like silver and gold have good antifungal efficiency. According to existing research the biosynthesized gold nanoparticles may penetrate and interrupt the mechanism of cell membrane synthesis, production of reactive oxygen species or biomolecular damage in the selected pathogenic organism. The one-way ANOVA test revealed that the zone of inhibition between various concentrations of AP-AuNPs and standard antibiotics (azithromycin) for bacterial strains showed significant difference (F=91.44; p<0.001) and fungal strains (*A. flavus* and *A. niger)* showed significant difference (F=91.44 and 87.10; p<0.001) respectively followed by the post hoc tukey test

(Table 1; $p<0.001$). The MIC was found to be significant with IC50 values of 14.19, 14.08 and 18.07 µg/ml respective strains such as *Aspergillus flavus*, *Aspergillus niger* and *Pseudomonas syringae* (Fig 11).

CONCLUSION

In most of the countries, agriculture is the mainstay of the economy. Gold nanoparticles have been extensively explored over the last few decades, and their usage in agriculture offers an alternative for pathogen control that could diminish our necessity on environmentally harmful fungicides and bactericides. Green synthesis of AugNPs is made simple and inexpensively using extracts from *Andrographis paniculata* leaves. Nano based endeavours should be formulated for their role in plant disease remedy owing to being a cost effective and ecofriendly substitute. Based on the experimental results we conclude gold nanoparticles have potential antimicrobial efficacy which can supports the shelf life of plants as well as disease management. In future we could develop new nano formulated drugs to combat plant pathogens in agricultural sectors.

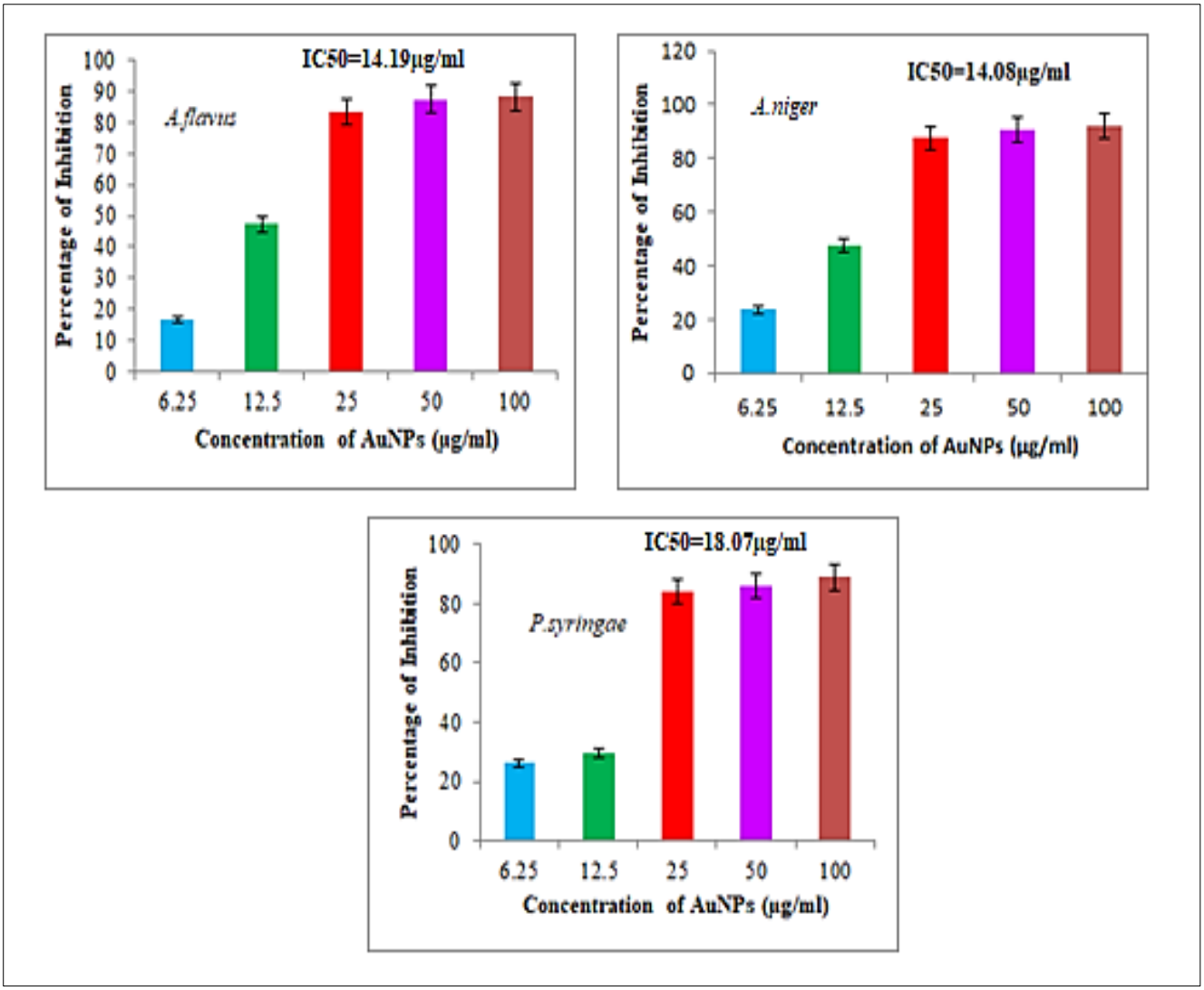

Fig 11 Minimum inhibitory concentration of AuNPs against selected plant pathogens

LITERATURE CITED

1. Mohseniazar M, Barin, M, Zarredar H, Alizadeh S, Shanehbandi D. 2011. Potential of microalgae and lactobacilli in biosynthesis of silver nanoparticles. *Bioimpacts* 1: 149-152.
2. Khan I, Saeed K, Khan I. 2019. Nanoparticles: Properties, applications and toxicities. *Arabian Journal of Chemistry* 12: 908-931.
3. Fontana DC, De Paula S, Torres AG, De Souza VHM, Pascholati SF, Schmidt D, Neto DD. 2021. Endophytic fungi: Biological control and induced resistance to phytopathogens and abiotic stresses. *Pathogens* 10(5): 570.
4. Moore D, Robson GD, Trinci AP. 2020. *21st Century Guidebook to Fungi*. Cambridge: Cambridge University Press.
5.Taubenhaus JL. 1920. A study of the black and yellow molds of ear-corn. *Texas Agric. Exp. Sta. Bulletin*. pp 270.
6. Pettit RE. 1984. Yellow mold and aflatoxin. *In*: Compendium of Peanut Diseases (Eds) Porter DM, Smith DH, Rodriguez-Kabana R, St. Paul MN: *The American Phytopathological Society*. pp 35-36.
7. Marsh PB, Bollenbacher K, San Antonio JP, Merola GV. 1955. Observations on certain fluorescent spots in raw cotton associated with growth of microorganisms. *Textile Res. Journal* 25: 1007-1016.
8. Anderegg RJ, Biemann K, Buechi G, Cushman M. 1976. Malformin C, a new metabolite of *Aspergillus niger*. *Jr. Amer. Chem. Society* 98: 3365-3370.

9. Sharma RC, Vir D. 1986. Post-harvest diseases of grapes and studies on their control with benzimidazole derivatives and other fungicides. *Pesticides* 20: 1415-1415-1986.
10. Sinha P, Saxena SK. 1987. Effect of treating tomatoes with leaf extract of *Lantana camara* on development of fruit rot caused by *A. niger* in presence of *Drosophila busckii*. *Indian Jr. Exp Biology* 25: 143-144.
11. Worrall EA, Hamid A, Mody KT, Mitter N, Pappu HR. 2018. Nanotechnology for plant disease management. *Agronomy* 8: 285.
12. Mani M, Pavithra S, Mohanraj K, Kumaresan S, Alotaibi SS, Eraqi MM, Gandhi AD, Babujanarthanam R, Maaza M, Kaviyarasu K. 2021. Studies on the spectrometric analysis of metallic silvernanoparticles (Ag NPs) using *Basella alba* leaf for the antibacterial activities. *Environ. Research*. pp 199.
13. Gandhi AD, Kaviyarasu K, Supraja N, Velmurugan R, Suriyakala G, Babujanarthanam R, Zang Y, Soontarapa K, Almaary KS, Elshikh MS, Chen TW. 2021. Annealing dependent synthesis of cytocompatible nano-silver/calcium hydroxyapatite composite for antimicrobial activities. *Arab. Jr. Chemistry* 14: 103404.
14. Rathnakumar SS, Noluthando K, Kulandaiswamy AJ, Rayappan JBB, Kasinathan K, Kennedy J, Maaza M. 2019. Stalling behaviour of chloride ions: A non-enzymatic electrochemical detection of A-Endosulfan using CuO interface. *Sens. Actuators B: Chemistry* 293: 100-106.
15. Li S, Al-Minsed FA, El-Serehy HA, Yang L. 2021. Green synthesis of gold nanoparticles using aqueous extract of *Mentha longifolia* leaf and investigation of its anti-human breast carcinoma properties in the *in vitro* condition. *Arab. Jr. Chemistry* 14: 102931.
16. McFarland AD, Haynes CL, Mirkin CA, Van Duyne RP, Godwin HA. 2004. Color my Nanoworld. *Jr. Chem. Education* 81: 544A.
17. Saqr AA, Khafagy ES, Alalaiwe A, Aldawsari MF, Alshahrani SM, Anwer MK, Khan S, Lila AS, Arab HH, Hegazy WAH. 2021. Synthesis of gold nanoparticles by using green machinery: characterization and *in vitro* toxicity. Nanomaterilas 2011: 11: 808.
18. Balasubramanian S, Kala SMJ, Pushparaj TL. 2020. Biogenic synthesis of gold nanoparticles using *Jasminum auriculatum* leaf extract and their catalytic, antimicrobial and anticancer activities. *Jr. Drug Deliv. Sci. Technology*. pp 57.
19. Nikaeen G, Yousefinejad S, Rahmdel S, Samari F, Mahdavinia S. 2020. Central composite design for optimizing the biosynthesis of silver nanoparticles using *Plantago major* extract and investigating antibacterial, antifungal and antioxidant activity. *Sci. Reports* 10(1): 1-16.
20. Prema P, Iniya PA, Immanuel G. 2016. Synthesis, characterization, antibacterial and synergistic effect of gold nanoparticles using *Klebsiella pneumoniae* (MTCC-4030). *RSC Advances* 6: 4601-4607.
21. Pal R, Panigrahi S, Battacharyya D, Chakraborti AS. 2013. Characterization of citrate capped gold nanoparticle -Quercetin complex: Experimental and quantum chemical approach. *Jr. Mol. Structure* 1046: 153-163.
22. Abdoli M, Arkan E, Shekarbeygi Z, Khaledian S. 2021. Green synthesis of gold nanoparticles using *Centaurea behen* leaf aqueous extract and investigating their antioxidant and cytotoxic effects on acute leukemia cancer cell line (THP-1). *Inorg. Chem. Communication* 129: 108649.
23. Devanesan S, AlSalhi MS. 2021. Green synthesis of silver nanoparticles using the flower extract of *Abelmoschus esculentus* for cytotoxicity and antimicrobial studies. *Int. Jr. Nanomedicine* 16: 3343-3356.
24. Zhao L, Wang Y, Zhao X, Deng Y, Li Q, Xia Y. 2018. Green preparation of Ag-Au bimetallic nanoparticles supported on graphene with alginate for non-enzymatic hydrogen peroxide detection. *Nanomaterials* 8(7): 507-519.
25. Ahmed A, Rauf A, Hemeg HA, Qureshi MN, Sharma R, Aljohani ASM, Alhumaydhi FA, Khan I, Alam A, Rahman MM. 2022. Green synthesis of gold and silver nanoparticles using *Opuntia dilleniid* Aqueous extracts: Characterization and their antimicrobial assessment. *Jr. Nanomaterials* 2022: 1-17.
26. Keskin C, Baran A, Baran MF, Hatipoglu A, Adican MT, Atalar MN, Huseynova I, Khalilov R, Ahmadian E, Yavuz O, Kandemir SI, Eftekhari A. 2022. Green synthesis, characterization of using *Gundelia tournefortii* leaf extract, and determination of their nanomedicinal (Antibacterial, Antifungal, and Cytotoxic) potential. *Jr. Nanomaterials.* 2022: 1-10.
27. Hemlata, Meena, PR, Singh AP, Tejavath KK. 2020. Biosynthesis of silver nanoparticles using *Cucumis prophetarum* aqueous leaf extract and their antibacterial and antiproliferative activity against cancer cell lines. *ACS Omega* 5(10): 5520-5528.
28. Adena SKR, Upadhyay M, Vardhan H, Mishra B. 2019. Development, optimization, and in vitro characterization of dasatinib-loaded PEG functionalized chitosan capped gold nanoparticles using Box-Behnken experimental design. *Drug Dev. Ind. Pharmacology* 44: 493-501.
29. Gao M, Sun L, Wang Z, Zhao Y. 2013. Controlled synthesis of Ag nanoparticles with different morphologies and their antibacterial properties. *Mater. Sci. Engineering C* 33: 397-401.
30. Ni Z, Gu X, He Y, Wang Z, Zou X, Zhao Y, Sun L. 2018. Synthesis of silver nanoparticle-decorated hydroxyapatite (HA@ Ag) poriferous nanocomposites and the study of their antibacterial activities. *RSC Advances* 8: 41722-41730.